MODELLING OF SPATIAL INFECTION SPREAD THROUGH HETEROGENEOUS POPULATION: FROM LATTICE TO PDE MODELS

by

Arvin Vaziry

Submitted in partial fulfillment of the requirements
for the degree of Master of Science

at

Dalhousie University
Halifax, Nova Scotia
December 2021

Table of Contents

List of Tables

List of Figures

Abstract

We derive a PDE model of the infection spread, which takes population density into account. This model is a continuum limit of agent-based model of human movement. Numerical simulations of the model show that dense population areas encounter higher probability of outbreak, which shows consistency with reality. We also investigate the effect of having large diffusion rate in the model. Our further studies show propagation of disease in the domain, which its speed varies with population density. We estimate this speed in the slow diffusion rate regime. Its propagation between two dense areas that are connected with a very low population density area is proven to be possible by our works. As a case example, we examine coronavirus spread in the Canadian province of Nova Scotia which enable us to verify our understanding of "tunneling" between two dense regions. Lastly, we propose several generalizations of the model towards future studies.

Chapter 1

Introduction

It is difficult to believe that the SARS-CoV-2 virus, which cannot be seen with naked eyes, in a quite short time could infect millions of people all over the world and could affect our lives deeply. Infectious disease severely threatens human life [1], and this pandemic may not be the last one. Due to the world population growth and the increasing necessity for people to be connected with each other, (hence the necessity for travelling, either local travels or long-distance ones) we may encounter worse situations in the future.

Epidemiology is the cornerstone of public health [2] and mathematical analysis and modelling has been central to infectious disease epidemiology [3]. Mathematical models can be used to link the biological process of transmission and the emergent dynamics of infection at the population level, which immediately leads to several useful results: the expected size of an epidemic and the critical level that is needed for an intervention to achieve effective disease control [3]. Therefore, it can be used to address both scientific hypotheses and disease-control policy questions [3]. Fundamental to the growing importance of mathematical epidemiology is the integration of mathematical models with statistical methods to estimate key parameters of these models and test hypotheses using available data [3]. There are various observations of spreading the infectious disease which give rise to important questions about the dynamic of this spread and accuracy of these models comparing to real observations. What is the role of people motion in the spread of disease? Can we state the condition that the spread of the pathogen result in epidemic, and what is its threshold? How fast the outbreak can hit different regions?

In the era of coronavirus, the ongoing public discussion frequently refers to the reproduction number R_0, as a (simple) single-number diagnostic that captures the entire epidemic for a given country or region; for a summary of mathematical discussions of this diagnostic, we refer the interested reader to [4, 5, 6]. In reality, R_0 is

a parameter which changes locally, a feature that has not only been realized during the COVID-19 pandemic (see, e.g., [7]), but indeed one that has been well-known for similar outbreaks of other diseases such as dengue [8]. For example, it is natural to expect that areas with high population density and/or limited public health measures are hit much harder than more rural areas, or regions with strict health controls (masking and distancing). This suggests the limited value of describing the entire population by a single reproduction number R_0. In light of such considerations, herein we are interested in modelling of how the spread of disease depends on local spatio-temporal circumstances. One of the key parameter affecting the disease spread is population density. Our aim is thus to develop a simple, potentially generalizable model which captures the effect of population density and local differences on overall epidemic spread.

At the heart of many epidemiology models and in the frame of this study as well, are the so-called compartmental models, consisting of various classes of individuals and their interactions. Compartmental models simplify the mathematical modelling of infectious diseases by assigning the population to different compartments or blocks. The first letter of these blocks' labels and their order determines the name of the model. People may progress between compartments and the order of the labels usually shows the flow patterns between the compartments. For example SEIS represents a model with compartments of susceptible (S), exposed (E), infectious (I), then susceptible again. Corresponding equations show the flow of population between different compartments of model. The more compartments would indicate more details of transition of people among them and definitely create more variables. Figure 1.1 shows an example of compartmental model with many different compartments, including hospitalized cases [9].

Among the many possibilities that have arisen not only in the context of COVID-19, but also earlier, we note the formulation of ODE models [10, 11, 12, 13], statistical models [11, 14], stochastic models [15], agent-based models [16, 17], spatial network models[14, 18] and partial differential equation (PDE) models [9, 19]; see also [16, 20] for reviews. Some of these works turn out to have a very deep influence on public thinking and policy [12, 17].

The focus of the present work will be on spatially-distributed models exploring

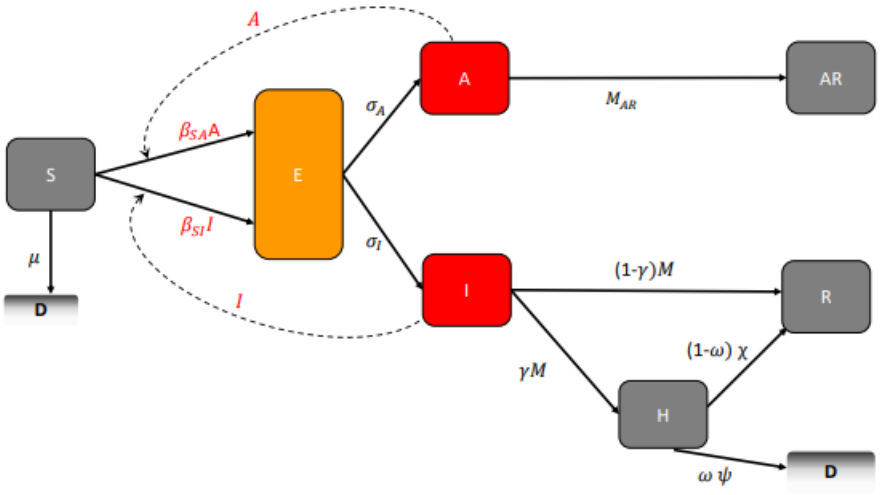

Figure 1.1: Schematic diagram of the SEAIHR model (Taken from [9]).

the evolution of the infection not only temporally but also spatially. Indeed, such models have a time-honored history, e.g., in the format of metapopulation models [21] and have been extensively used in the context of COVID-19 [22]. Such models have been used for a diverse host of countries including China [23, 24] and Spain [25, 26], while a comparison of different models developed, e.g., for the US can be found in the so-called COVID-19 Forecast Hub [1]. On the other hand, there exist also models that develop a PDE perspective such as [27, 28], in addition to earlier work by the present authors such as [9, 19] (see also references within these works).

Our aim in the present work is to complement the above approaches by means of a first-principles look into the development of the interaction between the different agents as they move through the spatial domain (and interact with each other). In so doing, we will develop a nonlinear dynamical lattice based approach, which can then be taken to the continuum limit, to yield a systematic PDE model that can be more suitable towards the modeling of COVID-19, as well as of other infectious diseases. Indeed, rather than incorporating standard processes such as diffusion and advection into an ODE SIR-type model, this perspective retrieves a nonlinear variant of diffusion which seems to us to be more well-suited to such epidemic settings. Additionally, a key advantage of the present model is that it enables a variety of generalizations to

[1]The relevant website is https://covid19forecasthub.org/doc/ensemble/.

account for effects of longer range interactions (and, of course, additional effects such as those, e.g., of age distribution of the pandemic impact). Such potential extensions will be highlighted along the way. It is also relevant to mention that both for reasons of concreteness, but also for practical ones related to the identifiability of the model [29] (which does not escape us as a central issue and a consistent source of concern about complex models), we opt within the present seed study to focus on the prototypical SIR-type model. Generalizations to more detailed models with a higher number of compartments will be evident, including also in connection to earlier work of some of the authors [9, 30].

Our presentation will be structured as follows. In chapter 2, after a brief introduction about SIR model, we will present the theoretical formulation of our model (and its potential extensions). In chapter 3, we will investigate how our model might change when diffusion is very large and we derive a set of new equations. In the next chapter, we will use our model to explore invasion waves and their respective speed. In the chapter 5, the onset of an infection outbreak will be examined. Finally, after briefly touching upon the case example of Nova Scotia in chapter 6, we conclude and present some future challenges in section 6. The contents of this thesis were submitted for publication [31].

Chapter 2

Theoretical formulation of the model

Choosing the appropriate number of compartments is the essential starting point. Deciding to consider more compartments results in more equations and more variables which increase the cost of simulations and analysis. Regarding our main goal, the simplest compartment model, or SIR seems to be promising, by which without struggling with many variables, we can study the role of population motion in the spread of disease.

In this chapter, after a brief introduction about SIR model, we will try to obtain continuum PDEs by starting from discretized model on a lattice problem.

2.1 SIR model

The SIR model is one of the simplest compartmental models, and many models are derivatives of this basic form. As its name indicates, this model consists of three main compartments. First compartment is Susceptible and the number of susceptible individuals is shown by S. When a susceptible and an infectious individual come into "infectious contact", the susceptible individual contracts the disease and transitions to the infectious compartment, which the number of infectious individuals is shown with I. These are individuals who have been infected and are capable of infecting susceptible individuals. The last compartment which is shown with R, indicates the number of removed (and immune) or deceased individuals. These are individuals who have been infected and have either recovered from the disease and entered the removed compartment or died. This compartment may also be called "recovered" or "resistant". The immunization period for those individuals who recovered from disease, comparing to time of our study, is long enough that they will not become susceptible again.

This model is reasonably predictive for infectious diseases that are transmitted from human to human, and where recovery confers lasting resistance, such as measles,

mumps and Covid-19.

For simplicity, we will deploy several assumptions:

1. Constant (closed) population size, N

2. Constant rates (e.g., transmission, removal rates)

3. No demographic changes (i.e., births and deaths)

4. Well-mixed population. A well-mixed population is one where any infected individual has a probability of contacting any susceptible individual that is reasonably well approximated by the average [32]. This is often the most problematic assumption but is easily relaxed in more complex models. [32]

Based on the definition we know that $N = S + I + R$. Hence, by the first assumption we can write:

$$\frac{dN}{dt} = 0 \tag{2.1}$$

Considering all above-mentioned assumptions, the SIR equations can be written as follows:

$$\begin{aligned} \frac{dS}{dt} &= -\frac{\beta}{N} SI \\ \frac{dI}{dt} &= \frac{\beta}{N} SI - \gamma I \\ \frac{dR}{dt} &= \gamma I \end{aligned} \tag{2.2}$$

where β is known as the effective contact rate, and γ is the removal rate.

Now, we can set up the main problem in order to derive the PDE equations that governs the spread of the disease.

2.2 Deriving continuum equations

By studying the SIR model, we could find the equations that show the transition of population between different compartments. Now we want to address this question that how the motion and interaction of population of different regions may lead to the spread of disease.

We start with an agent based model, with the aim of deriving a cellular automata model from it, and then consider its continuum limit to obtain a PDE system. A similar procedure was used in [33] to derive a spatio-temporal model of spreading of

illegal activity. We assume that individuals can get infected by going out of their home and traveling to new locations. However they don't just simply walk at random, or diffuse: after going out (e.g. say for shopping or work), they return to their original (base) location. For this purpose, we consider the lattice problem, one dimension problem with grid points, which can represent different regions within one city, different cities within one province, etc. People, either infected or susceptible, can travel between neighbourhood grid points. To start with, we assume that only susceptible individuals can travel, and with a constant rate α. Grid points are in equal distance of Δx from each other. The schematic of the problem can be shown as figure 2.1.

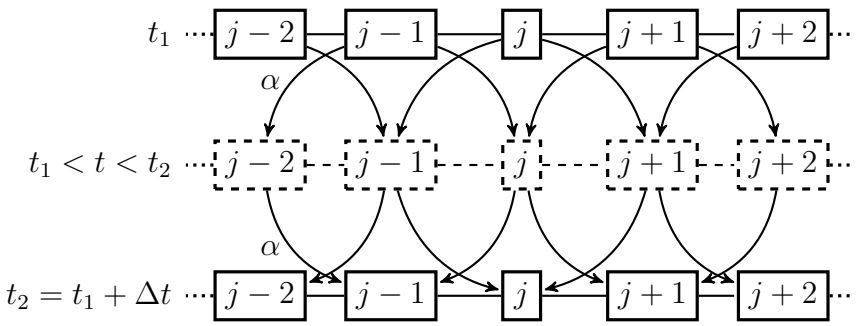

Figure 2.1: The schematic of people moving between different grid points within Δt. The middle row shows the transient situation. α is assumed to be constant for all grid points.

Consider a grid point, for example j, within a step time Δt. We assume that a fraction of susceptible individuals of this grid point will travel to neighbourhood grid points $j-1$ and $j+1$ (second row of figure 2.1), and they will return to their home grid point at the end of this step time (bottom row of figure 2.1). Hence, if we show the susceptible individuals of grid point j at time t with S_j^t, we can conclude that only $S_j^t(1-2\alpha)$ might have interactions with infected individuals of this grid point; αS_j^t would be exposed to infected ones at grid point $j-1$, and the same number would be exposed to infected ones at point $j+1$. Using SIR equations, we can write the equation for ΔI_j, new infected cases of grid point j, as follows:

$$\begin{aligned}\Delta I_j &= \Delta t\beta(S_j^t - 2\alpha S_j^t)I_j^t \\ &+ \Delta t\beta(\alpha S_j^t)I_{j-1}^t \\ &+ \Delta t\beta(\alpha S_j^t)I_{j+1}^t\end{aligned} \tag{2.3}$$

As discussed, the first term show the new infected cases due to the interaction between those individuals who didn't travel with infected ones at the same point. The next two terms term show new infected who returned to their home point after interacting with infected ones of neighbourhood points. For better understanding of equation (2.3), it can be rewritten as below:

$$\Delta I_j = \Delta t\beta S_j^t I_j^t + \Delta t\beta\alpha S_j^t(-2I_j^t + I_{j-1}^t + I_{j+1}^t) \tag{2.4}$$

We can estimate: $I(x,t) \approx I_j^t$ where $x = j\Delta x$, and hence we can write: $(I_{j-1}^t - 2I_j^t + I_{j+1}^t) = \Delta x^2 I_{xx}$. In the limit when $\Delta x \to 0$, $\Delta t \to 0$ and by disregarding higher orders of Δx we can write the equation as follows:

$$\Delta I = \beta(SI + \Delta x^2 \alpha S I_{xx}) \tag{2.5}$$

By defining:

$$D = \alpha(\Delta x)^2 \tag{2.6}$$

we can rewrite the continuum equation as follows:

$$\Delta I = \beta(SI + DSI_{xx}) \tag{2.7}$$

Now that we have the continuum equation for new infected cases, we can write new SIR equations as follows:

$$\begin{aligned}S_t &= -\Delta I = -\beta(SI + DSI_{xx}) \\ I_t &= \Delta I - \gamma I = \beta(SI + DSI_{xx}) - \gamma I \\ R_t &= \gamma I\end{aligned} \tag{2.8}$$

Note that unlike many other PDE models [27, 28, 34, 35], the "diffusion" term depends explicitly on the susceptible population density $S(x,t)$. Moreover, the "diffusion" enters into equation for S with a negative sign, whereas it has a positive sign in the equation for I.

Our assumption for the motion of people at the beginning of this section results in showing up new terms in the equation (2.7). This is a realistic assumption and consistent with our experience and observations during the pandemic of Covid-19. People leave their home, home town or home country for different purposes and at the end bring virus back to their origin. This is exactly what we try to show, the interaction of people with population of other regions which spread the disease and make an outbreak.

We can generalize our result by assuming that infected individuals can also travel. As figure 2.1 shows, for example, some of the infected population at point $j-2$ will travel to point $j-1$. This means that susceptible individuals of point j who will travel to point $j-1$, before returning to their main point might be exposed to those infected ones from point $j-2$, which increases the probability of getting infected. The same scenario will happen at point $j+1$, where those susceptible who travel from point j will be exposed to infected ones of point $j+2$ who will travel to point $j+1$. This ends up adding more positive term to the equation (2.3), as follows:

$$\begin{aligned}\Delta I_j = &\Delta t\beta(S_j^t - 2\alpha_S S_j^t)(I_j^t + \alpha_I(I_{j-1}^t + I_{j+1}^t - 2I_j^t)) \\ &+ \Delta t\beta(\alpha_S S_j^t)(I_{j-1}^t + \alpha_I(I_{j-2}^t + I_j^t - 2I_{j-1}^t)) \\ &+ \Delta t\beta(\alpha_S S_j^t)(I_{j+1}^t + \alpha_I(I_{j+2}^t + I_j^t - 2I_{j+1}^t)).\end{aligned} \tag{2.9}$$

Here α_S and α_I are travel rates for susceptible and infected individuals accordingly. Following the same steps as before, in the limit when $\Delta x \to 0$, $\Delta t \to 0$ and by disregarding higher orders of Δx we can obtain:

$$\Delta I = \beta(SI + \Delta x^2 \alpha_S SI_{xx} + \Delta x^2 \alpha_I SI_{xx}) \tag{2.10}$$

By defining $D_S = \alpha\Delta x^2$ and $D_I = \alpha\Delta x^2$, we can rewrite the equation (2.10):

$$\Delta I = \beta(SI + D_S SI_{xx} + D_I SI_{xx}) \tag{2.11}$$

This is equivalent to the equation (2.8) by taking $D = D_S + D_I$.

In the next chapters, we will conduct some experiments to study the numerical results and evaluate the accuracy of our approximations.

Chapter 3

Derivation of model when diffusion rate (D) is large

In this chapter we return to the equation (2.8), and we investigate how this equation may change for large diffusion rate, when $D \gg 1$.

To embark on, we expand S and I as follows:

$$S \sim S^0 + \frac{1}{D}S^1 + ... \quad , \quad I \sim I^0 + \frac{1}{D}I^1 + ... \tag{3.1}$$

By plugging (3.1) into (2.8), leading order equation in terms $O(D)$ can be obtained as $S^0 I^0_{xx} = 0$, or rather $I^0_{xx} = 0$. Considering Neumann boundary conditions, we can conclude that I^0 won't change in space and it only depends on time. After doing some simulations, as one see in the figure 3.1, we observe that $S(x,t)$ decreases independent of x as time evolves. Therefore we expect that S^0 depends on time and we rewrite S^0 in this way:

$$S^0(x,t) = S_0(x) + f(t) \tag{3.2}$$

Here S_0 is the initial distribution of people. For the next order, one can write:

$$I^0_t = \beta((S_0(x) + f(t))I^0 + (S_0(x) + f(t))I^1_{xx} + S^1 I^0_{xx}) - \gamma I^0 \tag{3.3}$$

We know that $I^0_{xx} = 0$. Therefore we can rewrite the equation (3.3) as follows:

$$I^1_{xx} = \frac{I^0_t}{\beta(S_0(x) + f(t))} - I^0 + \frac{\gamma I^0}{\beta(S_0(x) + f(t))} \tag{3.4}$$

By integrating on the domain $x \in (0, L)$ from both sides of (3.4), the left hand side becomes zero, due to the boundary conditions. Recalling our previous result that I^0 is only a function of time, we can conclude that:

$$0 = \frac{1}{\beta}I^0_t \int_0^L \frac{1}{S_0(x) + f(t)}dx - I^0 \int_0^L dx + \frac{\gamma}{\beta}I^0 \int_0^L \frac{1}{S_0(x) + f(t)}dx \tag{3.5}$$

Hence we can rewrite the equation as follows:

$$I^0_t = \beta \frac{I^0}{1/L \int_0^L \frac{1}{S_0(x)+f(t)}dx} - \gamma I^0 \tag{3.6}$$

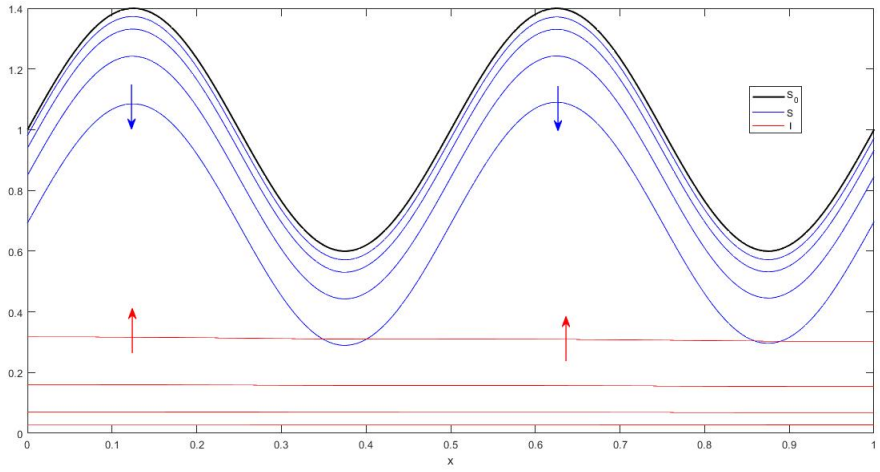

Figure 3.1: The graph of S and I as time evolves, in the case where diffusion is very large ($D \gg 1$), $\beta = 0.5$.The initial population is assumed to be $S_0(x) = 1 + 0.4sin(4\pi x)$ and initial infected function to be $I_0(x) = 0.01exp(-100x^2)$

The quantity $\left(\frac{1}{L}\int_0^L (S_0(x) + f(t))^{-1}\right)^{-1}$ is called the harmonic average of $(S_0(x) + f(t))$. Now we can follow the same steps for the equation of S_t^0, and by considering the equation (3.2), the equation for the O(1) can be written as follows:

$$f_t = -\beta\left((S_0(x) + f(t))I^0 + (S_0(x) + f(t))\, I_{1xx} + S_1 I_{0xx}\right) \tag{3.7}$$

By plugging the equation (3.4) into (3.7):

$$f_t = -\beta\left((S_0(x) + f(t))\, I_t^0 + 1/\beta I_t^0 - (S_0(x) + f(t))\, I_0 + \gamma/\beta I^0\right) \tag{3.8}$$

and finally by substituting the (3.6), we can obtain a new equation:

$$f_t = -\beta \frac{1}{1/L\int_0^L \frac{1}{S_0(x)+f(t)}dx} I^0 \tag{3.9}$$

which is independent of x.

As shown, the original PDE equations (2.8) has reduced to ODE equations (3.6) and (3.9). We obtained $f(t)$ from both the numerical discretization of the main equation (2.8) (with D=1) and asymptotics (3.6) and (3.9). The result of a simulation for initial population of $S_0(x) = 1 + 0.4sin(4\pi x)$, initial infected cases of $I_0(x) = 0.01exp(-100x^2)$ and $\beta = 0.5$ is depicted in the figure 3.2. The small difference between asymptotic and full numerical solution guarantees our assumption and observations.

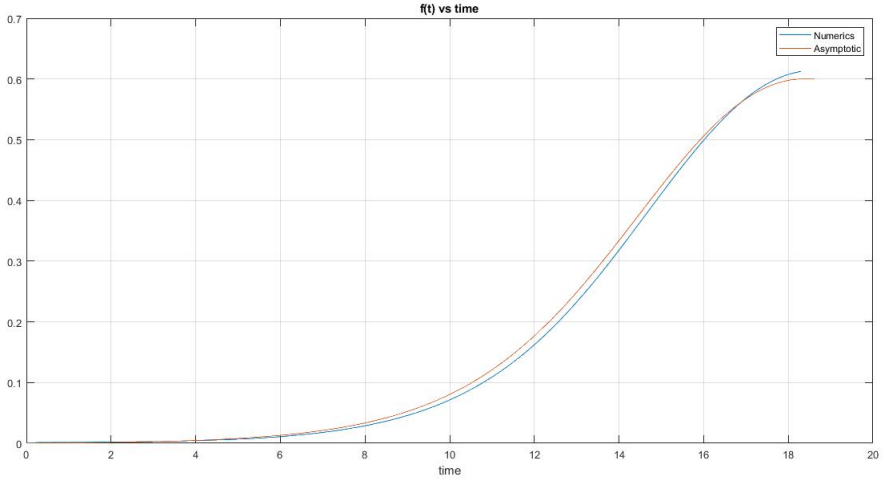

Figure 3.2: The graph of f(t) against time.

Although we could derive the asymptotic equations and do analysis, the earlier assumption of $D \gg 1$ doesn't have a physical interpretation. If we review the equation (2.6), where we defined D, it can be understood that there is certain restrictions by the constants in the equation. α represents the ratio of people who travel, and hence its maximum is 1. The other term in the definition of D is the distance of grid points, Δx, which cannot exceeds from a certain value, otherwise the descritized model may fail to reflect the reality. Therefore the minimum value of D is zero and its max is bounded by the maximum of $(\Delta x)^2$ or maximum distance of grid points that doesn't hurt the validity of numerical solution.

Chapter 4

Examination of an invasion wave

One of the main effects of introducing a spatial dimension, is that the infection typically propagates from its origin. When the movement is sufficiently slow, this propagation happens in a wave-like fashion. The first experiment we can investigate is studying in front of the wave of outbreak, when we have very small infected cases and negligible recovered cases. In the following, after deriving the equations, we will try to find some asymptotic solutions. At the end, we compare asymptotic solution and real results.

4.1 Set up the problem

We expect to have negligible recovered cases in font of the wave. Therefore we can approximate $S(x,t)$ as follows:

$$S(x,t) \approx S_0(x) - I(x,t) \tag{4.1}$$

In which, S_0 indicates the initial population. By plugging equation (4.1) into the equation (2.8), one can get:

$$I_t = \beta(S_0 - I)(I + DI_{xx}) - \gamma I \tag{4.2}$$

which is quite similar to KPP equation. If we consider that we have few infected cases at the front of the wave, we can disregard higher order terms of I, which means we can rewrite (4.2):

$$I_t \approx \beta D S_0 I_{xx} + (\beta S_0 - \gamma) I \tag{4.3}$$

In the following sections, after a brief introduction about KPP-Fisher equation, we will try to find an asymptotic solution for the speed of propagation of the disease.

4.2 KPP-Fisher equation

One-dimensional reaction-diffusion equations of the form:

$$u_t = u_{xx} + f(u), \quad t > 0, \quad x \in (-\infty, +\infty) \tag{4.4}$$

where $f(u)$ is a sufficiently smooth function of u, are used to model phenomena that occur in many areas of science and engineering [36]. One of the, arguably, simplest settings exhibiting wave propagation is the context of KPP-Fisher equation, modelling propagation of invasive species inside a favorable medium (see, e.g., [37] for a review):

$$u_t = du_{xx} + ru - su^2 \tag{4.5}$$

The travelling-wave solution has the form $u(x,t) = U(x - ct)$ where U satisfies the corresponding co-traveling ordinary differential equation (ODE):

$$-cU' = dU'' + rU - sU^2 \tag{4.6}$$

We seek a wave propagating from left to right, so that $U(z) \to 0$ as $z \to +\infty$, and $U \to r/s$ as $z \to -\infty$. Following the relevant standard theory and linearizing at the front of the wave ($z \to +\infty$), we can seek a solution of the form:

$$U(z) \sim e^{-\lambda z} \quad , \quad as \quad z \to +\infty \tag{4.7}$$

which yields a dispersion relationship between the speed c and the decay rate λ of the form:

$$c = d\lambda + \frac{r}{\lambda} \tag{4.8}$$

The minimum speed of propagation is obtained by minimizing equation (4.8) over all admissable decay rates $\lambda > 0$, which yields:

$$c_{min} = 2\sqrt{dr} \tag{4.9}$$

Numerical experiments confirm that the speed of propagation approaches c_{min} for a wide range of initial conditions, so long as $u(x,0)$ decays "sufficiently fast" as $x \to \infty$. This is a well-known feature of the KPP-Fisher equations [37, 38]. Note that this speed only depends on linear terms in the equation (4.8) (i.e, it is independent of the value of s). Now suppose that the parameters d, r are functions of space x. If they vary sufficiently slowly, we expect that the speed of propagation will still be well approximated by the equation (4.9). This is the so-called adiabatic approximation.

4.3 The asymptotic speed of propagation

The spread of an infectious disease looks like a wave propagating through the space. For the special case discussed in previous section, which can be observed in front of the wave with very small infected individuals, we assume that the motion is sufficiently slow (or rather $D \ll O(1)$)). By these assumption we want to linearize the equation at the front of the wave, like Fisher and KPP equation:

$$I(x,t) = e^{\lambda(x-ct)} \tag{4.10}$$

Hence the derivatives of $I(x,t)$ can be determined:

$$\begin{aligned} I_t &= -c\lambda e^{\lambda(x-ct)} \\ I_{xx} &= \lambda^2 e^{\lambda(x-ct)} \end{aligned} \tag{4.11}$$

We need to find c to determine the speed of propagation. Therefore, by plugging equations (4.10), (4.11) into the (4.2) and disregarding higher orders of I, one can get:

$$-c\lambda e^{\lambda(x-ct)} = \beta S_0 e^{\lambda(x-ct)} + \beta S_0 D e^{\lambda(x-ct)} - \gamma e^{\lambda(x-ct)} \tag{4.12}$$

By further simplifications and rewriting the equation for c, we may get:

$$c = -\frac{\beta S_0 - \gamma}{\lambda} - \beta S_0 D\lambda \tag{4.13}$$

At this point, we want to determine the minimum of c as a function of λ. By taking derivative of (4.13) with respect to λ, we may get the following equation:

$$\frac{\beta S_0 - \gamma}{\lambda^2} - \beta S_0 D = 0 \tag{4.14}$$

Which means that for $\lambda = \pm\sqrt{\frac{\beta S_0 - \gamma}{\beta S_0 D}}$ we have the optimum points, and by considering the direction of propagation, we can obtain the minimum speed as follows:

$$c_{min} = 2\sqrt{\beta S_0 - \gamma}\sqrt{\beta S_0 D} \tag{4.15}$$

In the following we will compare the approximate solution of (4.15) and full numerical solution.

4.4 Numerical Experiment

We run some experiment for different choices of initial population and compare the results of full numerical simulation with the result of (4.15).

We consider a lattice problem on $x - axis$ from $x = 0$ to $x = 1$, with $N = 200$ grid points. In this experiment, we investigate 2 different initial population, $S_0 = 1 + 0.4sin(4\pi x)$ and $S_0 = 1 + 0.7sin(4\pi x)$. We set the same constant values of $D = 0.0001$, $\beta = 0.5$, $\gamma = 0$ and the time interval of $\Delta t = 0.01$. for both initial densities.

As it is shown in the figure 4.1, the minimum speed is a relatively good approximation, especially when there is small changes in the population density. As the density changes more, this approximation fails and errors become larger.

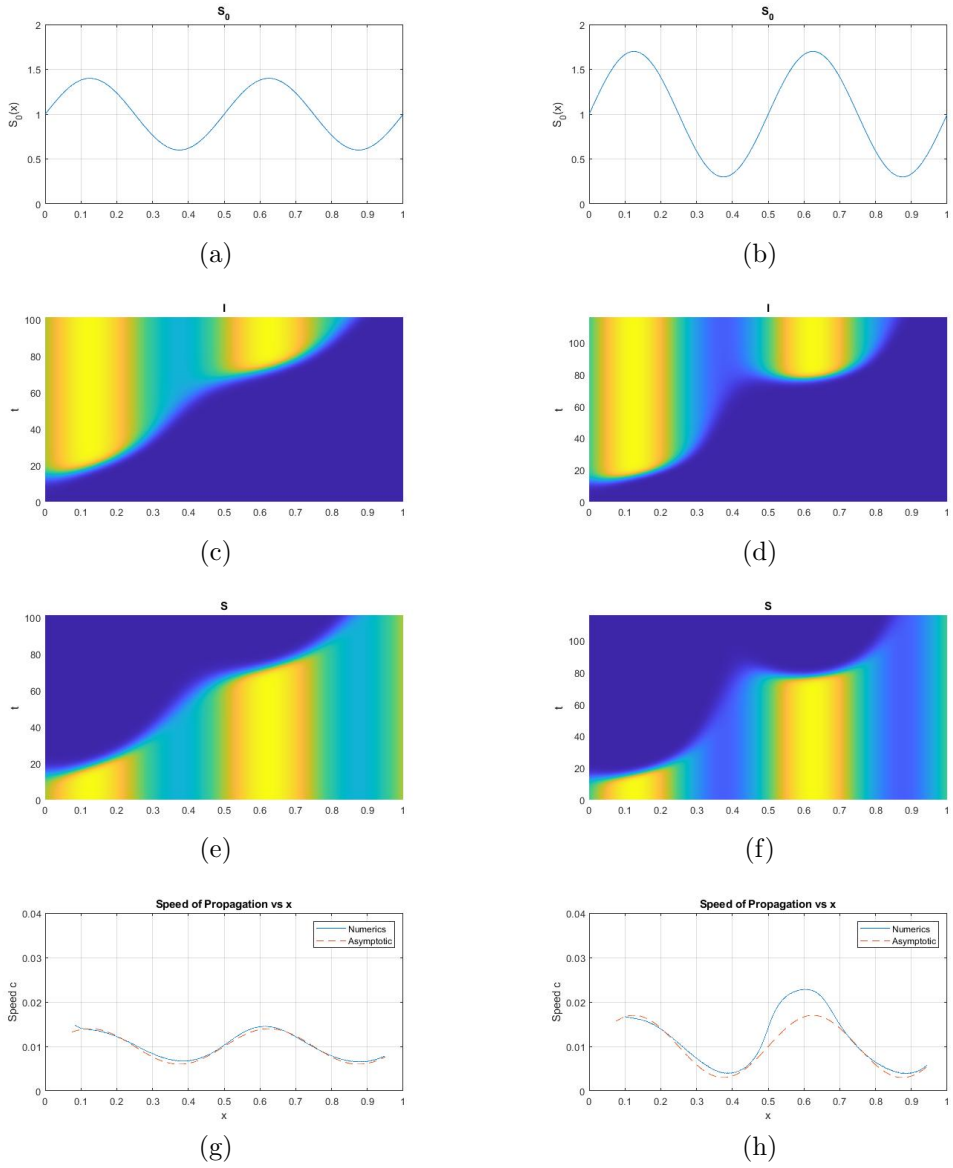

Figure 4.1: Simulation of an infection wave propagating through a heterogeneous population, for two initial densities. The left column indicates the results for $S_0(x) = 1 + 0.4sin(4\pi x)$, and the right column indicates ones for $S_0(x) = 1 + 0.7sin(4\pi x)$. The graph of these two initial functions has been depicted in the first row. Next two rows show the space time plot of susceptible and infected population density. The Last row shows the speed c of the wave as a function of wave position x, comparing numerical result to the asymptotic results.

Chapter 5

The onset of outbreak

In this chapter we want to investigate the conditions that lead to an outbreak. In the following sections, after linearizing derived equations, we will try to find corresponding eigenvalue problem that help us to find the threshold of outbreak. The equation (2.8) admits a trivial solution with $I(x,t) = 0$ and $S(x,t) = S_0(x)$, in which $S_0(x)$ describes the initial population distribution. In this case, outbreak won't happen. At the onset of the outbreak, we may assume that $I(x,t) \ll 1$. Linearizing (2.8) leads to an equation for I only of the form equation (4.3). Looking for solutions of the form $I(x,t) = e^{\lambda t}\phi(x)$, we obtain an eigenvalue problem:

$$\frac{\lambda + \gamma}{\beta S_0(x)}\phi = D\phi_{xx} + \phi \tag{5.1}$$

In the following sections we will consider different regimes and we will try to find the corresponding threshold.

5.1 Threshold of outbreak when diffusion is very small

To embark on, we consider the limit $D = 0$. In this case, each point x in space evolves separately, and the eigenvalues λ are given by $\lambda \sim \beta S_0(x) - \gamma$. The outbreak is therefore prevented when $\beta S_0(x) < \gamma$ for all x, or $\gamma > \gamma_c$, where:

$$\gamma_c = \beta \max_x S_0(x) \tag{5.2}$$

More generally, we define γ_c to be a threshold value of the decay parameter γ, corresponding to the zero-eigenvalue of (5.1). Namely, γ_c satisfies:

$$\frac{\gamma_c}{\beta S_0(x)}\phi = D\phi_{xx} + \phi \tag{5.3}$$

The outbreak occurs if and only if $\gamma < \gamma_c$. For general $S_0(x)$ and D; the equation (5.3) does not have an explicit solution. However we expect γ_c to approach the value (5.2) as $D \to 0$. We now derive the corrections to (5.2) in the limit of small but

non-zero $D : 0 < D \ll 1$, using asymptotic analysis. We expect the outbreak to first occur near the maximum of S_0. Let x_m be the point at which S_0 has its maximum. As such, we expand:

$$x = x_m + \varepsilon y \tag{5.4}$$

where ε is a small constant to be determined. Near x_m, we can write:

$$S_0(x) \sim A(1 - B\varepsilon^2 y^2) + O(\varepsilon^3) \tag{5.5}$$

where $A = S0(x_m), AB = -S_0''(x_m)/2$; and we expand $1/S_0(x) = (1 + B\varepsilon^2 y^2)/A$. Hence, we can rewrite equation (5.3) as:

$$\frac{\gamma_c}{A\beta}(1 + B\varepsilon^2 y^2)\phi \sim D\varepsilon^{-2}\phi_{yy} + \phi \tag{5.6}$$

We now choose ε so that $B\varepsilon^2 = D\varepsilon^{-2}$. In other words, we set:

$$\varepsilon := D^{1/4}B^{-1/4} \tag{5.7}$$

Assuming ε is small, to the leading order we obtain an eigenvalue problem:

$$\phi_{yy} - y^2\phi = \mu\phi, \qquad y \in \mathbb{R} \tag{5.8}$$

with:

$$\mu = (\frac{\gamma_c}{A\beta} - 1)D^{-1/2}B^{-1/2} \tag{5.9}$$

Equation (5.8) is a well-known quantum-harmonic oscillator whose eigenfunctions are given in terms of Hermite polynomials. The corresponding eigenvalues are given by:

$$\mu = 1, 3, 5, 7, ...$$

The smallest eigenvalue is $\mu = 1$. By plugging that into equation (5.9), we obtain the following formula for the threshold value of γ_c:

$$\gamma_c = S_0(x_m) - D^{1/2}(-S''(x_m)/2)^{1/2} + O(D). \tag{5.10}$$

For example, take $S_0(x) = a + sin(\pi x)$, $\beta = 1$, $x \in (0, 1)$. Then the maximum occurs at $x_m = 0.5$, and we obtain:

$$\gamma_c \sim 1 + a - D^{1/2}\pi(1 + a)^{1/2}2^{-1/2} \tag{5.11}$$

D	0.01	0.005	0.0025	0.00125
γ_c for numerics (5.3)	0.7778	0.8389	0.8871	0.9206
γ_c for asymptotics (5.11)	0.7686	0.8429	0.8889	0.9214
Relative error	1.18%	0.47%	0.20%	0.093%

Table 5.1: Comparison of numeric and asymptotic results of γ_c for different values of D. Initial population is assumed to be $S_0(x) = sin(\pi x)$, $x \in (0, 1)$ and $\beta = 1$.

Table 5.1 compares the formula (5.11) with the fully numerical solution of the eigenvalue problem (5.3), in the case of $a = 0$, for a couple of values of D.

After considering the case when we have a maximum of $S_0(x)$ within the boundary, now we want to investigate the case when we have a max on the boundary. Using the same expansion as (5.4), near x_m we can write:

$$S_0(x) \sim A(1 - B\varepsilon y) + O(\varepsilon^2) \tag{5.12}$$

where $A = S_0(x_m), AB = -S_0'(x_m)$; and hence we can write $1/S_0(x) = (1 + B\varepsilon y)/A$. We expect the leading order of γ_c to be the same as equation (5.2), and we can expand it as follows:

$$\gamma_c = \beta A(1 - \varepsilon\gamma_1) \tag{5.13}$$

By plugging equations (5.12) and (5.13) into the equation (5.3), we can write:

$$(1 - \varepsilon\gamma_1)(1 + B\varepsilon y)\phi \sim D\varepsilon^{-2}\phi_{yy} + \phi \tag{5.14}$$

We now choose ε so that $B\varepsilon = D\varepsilon^{-2}$. In other words, we set:

$$\varepsilon := D^{1/3}B^{-1/3} \tag{5.15}$$

Now the eigenvalue problem in the order of ε can be obtained as:

$$\phi_{yy} - (y - \frac{\gamma_1}{B})\phi = 0, \quad y \in \mathbb{R} \tag{5.16}$$

Now we define a new variable $\hat{y} = y - \frac{\gamma_1}{B}$. We can rewrite the equation (5.16) in terms of new variable:

$$\phi_{\hat{y}\hat{y}} - \hat{y}\phi = 0, \qquad \hat{y} \in \mathbb{R} \tag{5.17}$$

Equation (5.17) is a well-known Airy equation and its general solution can be written in terms of airy functions $\phi(\hat{y}) = aAi(\hat{y}) + bBi(\hat{y})$. Now we need to define new

D	0.01	0.005	0.0025	0.00125
γ_c for numerics (5.3)	0.7767	0.8389	0.8604	0.8895
γ_c for asymptotics (5.19)	0.7805	0.8258	0.8617	0.8903
Relative error	0.490%	0.268%	0.152%	0.088%

Table 5.2: Comparison of numeric and asymptotic results of γ_c for different values of D. Initial population is assumed to be $S_0(x) = 1 - x$, $x \in (0, 1)$ and $\beta = 1$.

boundary conditions as well. Boundary conditions in terms of x are $\phi'(x_m) = \phi'(L) = 0$. By changing variable to $\hat{y}$, new boundary conditions become $\phi'(-\frac{\gamma_1}{B}) = 0$, and $\phi'(\infty) = 0$. Considering the latter condition and the fact that ϕ is bounded, $Bi(\hat{y})$ cannot be part of the solution. Therefore the solution will be $\phi(\hat{y}) = aAi(\hat{y})$. We know that $\phi'(-\frac{\gamma_1}{B}) = 0$. Considering the smallest eigenvalue, which corresponds to first root of derivative of $Ai(\hat{y})$, and solving for γ_c, we will obtain:

$$-\frac{\gamma_1}{B} \approx -1.0188 \tag{5.18}$$

By substituting γ_1 in the equation (5.13), the threshold can be obtained as follows:

$$\gamma_c \sim \beta S_0(x_m)(1 - 1.0188 D^{1/3}(-S_0'(x_m)/S_0(x_m))^{2/3}) \tag{5.19}$$

For example, take $S_0(x) = 1 - x$, $\beta = 1$, $x \in (0, 1)$. Then the maximum occurs at $x_m = 0$, and we obtain:

$$\gamma_c \sim 1 - 1.0188 D^{1/3} \tag{5.20}$$

Table 5.2 compares the formula (5.20) with the fully numerical solution of the eigenvalue problem (5.3) for different values of D.

5.2 Threshold of outbreak when diffusion is very large

Let us also study the asymptotics in the limit of large D, on the domain $x \in [0, L]$ with Neumann boundary conditions $\phi'(0) = \phi'(L) = 0$, which yields $\phi_0(x) = const.$ By scaling, we may then take $\phi_0 = 1$. The next-order equation for ϕ_1 then becomes:

$$\frac{\gamma_c}{\beta S_0(x)}\phi = D\phi_{1xx} + 1 \tag{5.21}$$

We then integrate both sides on the domain to obtain:

$$\gamma_c \sim \beta \left(1/L \int_0^L \frac{1}{S_0(x)} dx\right)^{-1} \quad , \quad D \gg O(1) \tag{5.22}$$

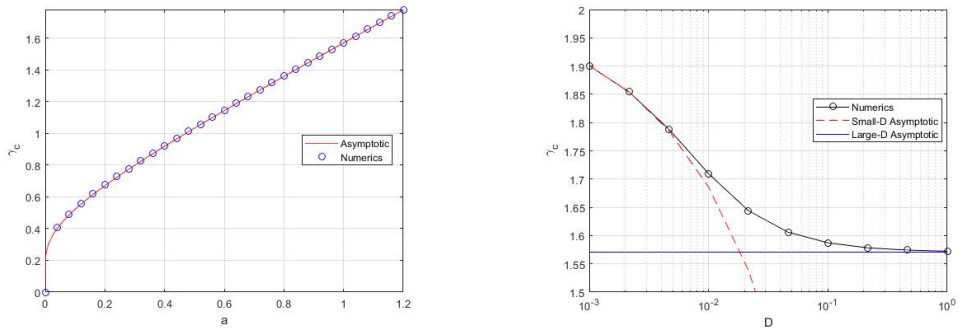

(a) (b)

Figure 5.1: (a):Threshold for outbreak γ_c in the limit of "large" D. Here, D=1 and $S_0(x) = a + sin(\pi x), x \in (0,1), \beta = 1$. The numerical solution of equation (5.3) and asymptotic given by equation (5.21) are both shown. They are indistinguishable, with relative error less than 0.1%.(b): Threshold as a function of D with $S0(x) = 1 + sin(\pi x)$: Small and large- D asymptotic are also shown.

in which the quantity $\left(\frac{1}{L}\int_0^L (S_0(x))^{-1}\right)^{-1}$ is called the harmonic average of $S_0(x)$. For example, take $S_0(x) = a + sin(\pi x)$ with $x \in (0,1)$. Then equation (5.21) integrates to:

$$\gamma_c \sim \begin{cases} \frac{\pi\sqrt{1-a^2}}{\log(1+\sqrt{1-a^2}-\log(1-\sqrt{1-a^2})}, & 0 < a < 1 \\ \pi/2, & a = 1 \\ \frac{\pi\sqrt{1-a^2}}{\pi-\arctan\left((a^2-1)^{-1/2}\right)}, & a > 1 \end{cases} \tag{5.23}$$

Figure 5.1 (a) compares the asymptotic (5.21) with full numerical simulations of (5.3) for a wide range of a, and with $D = 1$. Despite a relatively small value of D, the agreement is excellent over the entire range of a (within 0.1%). In 5.1 (b), we fix a = 1 and vary D; as can be seen, both large- and small- D asymptotics agree very well with full numerics.

Finally, note that for constant population density S_0, the theshold γ_c defined by (5.3) is independent of D, and both equation (5.10) and (5.22) yield $\gamma_c = \beta S_0$. One might naively expect that in the large-D limit, S_0 would be replaced by the arithmetic average of $S_0(x)$. However our analysis shows that the more appropriate formula is to take a *harmonic* average of $S_0(x)$ as in (5.22).

Chapter 6

Indicative observation from Covid-19 in Nova Scotia and "tunneling"

As a case study, consider the Canadian province of Nova Scotia where some of the authors of this paper reside. It has a population of about 1 million, with slightly less than half of those living in Halifax Regional Minicipality (HRM: the city of Halifax and surrounding area). The second-biggest town is Sydney (see map) with a population of 30,000. Much of the rest of the province has relatively low population density. Nova Scotia managed to completely suppress the initial outbreak in the spring of 2020 using very strict stay-at-home orders and border controls. Any visitor required a strict self-isolation quarantine of 2 weeks upon entry. As a result, there were very few locally-transmitted cases up until April 2021; stringent health measures managed to extinguish the few localized outbreaks that did occur before they spread.

Figure 6.1 shows the daily COVID case numbers for Nova Scotia. In total, as of July 2021, Nova Scotia had about 5800 cases, which is about 0.6% of the total population of 1 million. About 70% of these cases occurred during the "third wave" in April-June, 2021. Very few cases occurred in-between the three waves – and most of those were travel-related in quarantine (i.e., not involving community spread). Although less than half of NS population lives in HRM, it was responsible for 79% of the cases overall, and 81% of the cases in the third wave. Another 10.5% of cases occurred in Sydney, about 400km (4.5 hours drive) from Halifax, having a population of 30,000. Together, HRM and Sydney were responsible for over 90% of all infections, despite having about half of the overall population of the province. Despite its relatively smaller size, the infection rate in Sydney was about 2.5 times that of Halifax during the third wave.

The main takeaway lesson from this brief data summary, in connection to the qualitative model features discussed herein, is that the rate of infection is much higher in denser urban regions than the rest of Nova Scotia, which is mainly rural with low

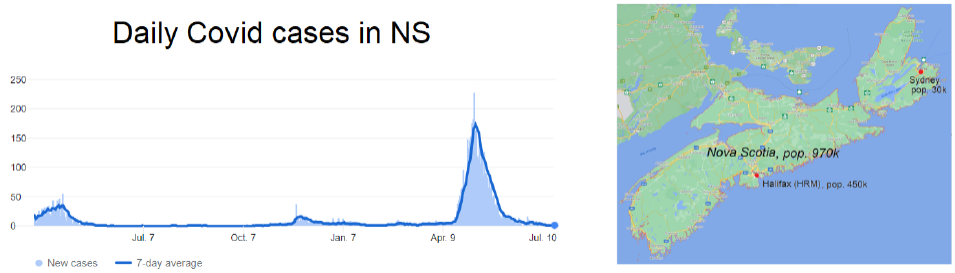

Figure 6.1: Daily COVID-19 cases for the Province of Nova Scotia. Around 80% of the cases occurred in the Halifax Regional Minicipality, which contains about 50% of the population of Nova Scotia.

population density. This is indeed consistent with our model and its corresponding observations. In addition, due to stringent health measures, it is likely that the epidemic in most of the regions of Nova Scotia did not spread – even during the third peak – as almost all infections came from HRM and Sydney – the two biggest population centers in Nova Scotia. Despite strict travel restrictions (even inter-provincial travel was banned during the third wave in May 2021), the infection was able to "tunnel through" the rural areas from HRM to Sydney.[1]

Motivated by the above observations, we now show that our model can reproduce, at least qualitatively, a "tunneling-through" effect, where the infection can spread between two regions of locally positive growth, even when separated by a "buffer zone" of negative growth (i.e., infection suppression). Consider a sample simulation as shown in Figure 6.2, with $S_0 = S_0(x) = 1.3 + cos(2\pi x)$ with $x \in (0, 1.5)$ and $\beta = \gamma = 1$. Locally (in the limit of $D = 0$), the infection is suppressed in the middle region $x \in (0.298, 0.701)$ as well as for $x > 1.298$ where $S_0(x)\beta < \gamma$, and grows to the left and to the right of that region. We initially introduce the infection near the left boundary of $x = 0$. The outbreak then takes over the entire left region $0 \leq x \leq 0.298$ by the time $t = 20$. Then for a relatively long time $20 < t < 100$, nothing appears to

[1]It is also interesting to note that there are other significant population centers closer to HRM that did not see anything near the size of outbreak in Sydney. This includes the towns of Truro (pop. 23000, one hour drive from Halifax) and New Glasgow (pop. 19000, 2 hours drive from Halifax) that did not see any significant outbreaks during the third wave. The outbreak in Sydney started with a hockey game, when kids and families from Halifax visited Syndey for a hockey tournament at the onset of the third wave, a potential superspreader event. At the end of the day, our simple model is insufficient to make predictions at such localized detail; much of the outbreaks are driven by random events and the luck of the draw, which our deterministic model is not designed in this first installment thereof to deal with. This is naturally an intriguing challenge for further work.

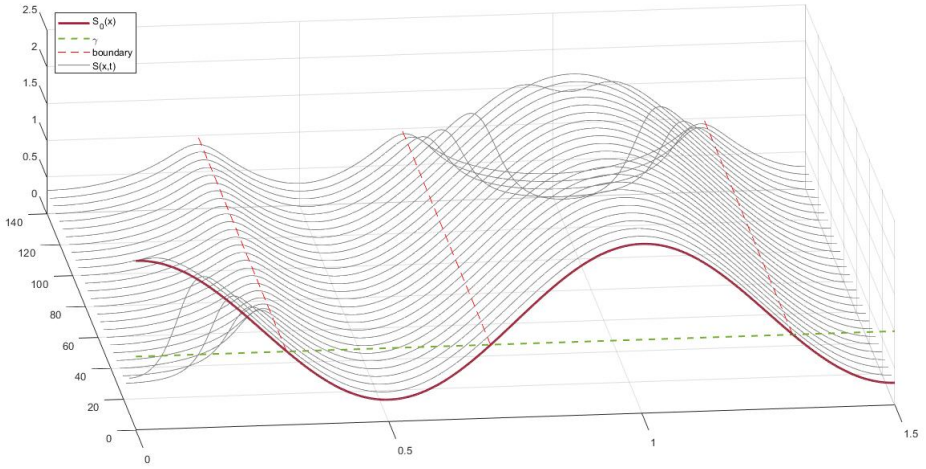

(a)

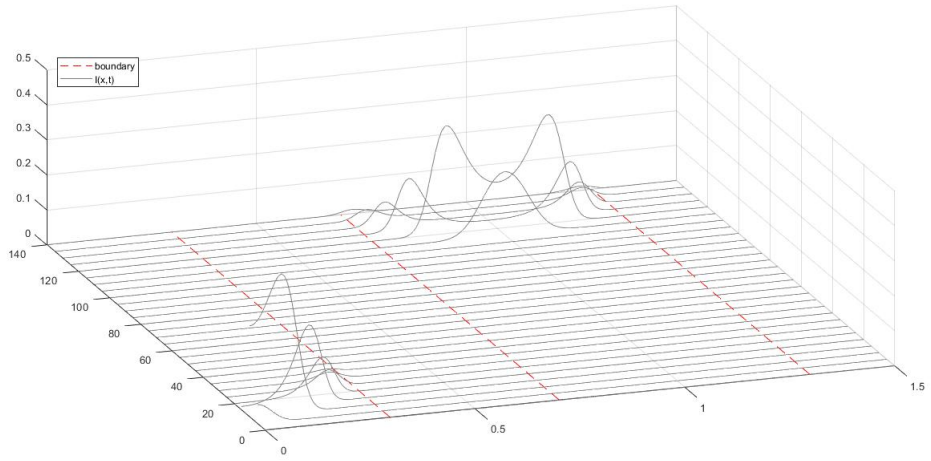

(b)

Figure 6.2: Infection "tunneling" through a barrier. Initial conditions was taken to be $S_0 = S_0(x) = 1.3 + cos(2\pi x)$ with $\beta = \gamma = 1$ and $x \in (0, 1.5)$. Without spatial interactions ($D = 0$), the disease is suppressed in the middle region $x \in [0.298, 0.701]$ as well for $x > 1.298$. Here, we take $D = 0.00005$. The disease is introduced at $t = 0$ at the left end $x = 0$; corresponding to initial conditions $I(x, 0) = 0.001e^{-1000x}$. An infection wave propagating to the right is initially observed, but appears to die out around $t \approx 30$ as it hits the buffer region at $x \approx 0.3$. However it is able to "tunnel through" the buffer region, re-appearing at $x = 1$ (where S_0 has its maximum) when $t \approx 90$, then propagating from there to the rest of the infectious region $x \in [0.7, 1.3]$.

happen. But eventually at around $t \approx 100$, the infection manages to "jump" over to the right region and re-appears at $x = 1$ (where $S_0(x)$ has its maximum), then spreads from there both to the left and to the right until the entire region $0.701 \leq x \leq 1.298$ is infected. It is interesting to note that when the infection re-appears at $t \approx 100$, it does so at $x = 1$ rather than $x \approx 0.7$. The reason merits further investigation, but roughly speaking, this happens because the local growth rate of infection is given roughly by $S_0(x)\beta = \gamma$, and is the highest at the maximum of $S_0(x)$.

Chapter 7

Conclusion

The content of this thesis were submitted for publication [31].

We have presented a model of spatio-temporal infection spread. We have started from a lattice variant of the problem and considered a first-principles inclusion of mobility according to which people move to new, adjacent locations (for work, shopping or other purposes), get infected and return to their base in that new infected state. The model allows for extensions whereby the mobility is to different locations (rather than to adjacent bins) with a presumably decaying over distance kernel. The latter constitutes an interesting variant of the current model relevant to examine in future work. Considering the continuum limit of the considered cellular automaton, we obtained a PDE (2.8) with state-dependent diffusion terms. Essentially, the scope of our work is to advocate the relevance of consideration of such terms, in addition to local ones and, arguably, instead of regular diffusion processes in this setting. The key assumption in our modelling is that while individuals move around, they don't diffuse, while infection does. While numerous PDE models exist in epidemiology (see, e.g., [9, 19, 27, 28, 34] for a sample), most assume either constant diffusion, or diffusion that is prescribed to be spatially-dependent. By contrast, we present a first-principles derivation of equation (2.8) from the underlying cellular automata representation of the basic infection mechanisms. Our model naturally leads to a diffusion that scales with the current number of susceptibles. We also investigated the special case when diffusion rate is very large. Our experiments showed that the PDE model can be written as a system of ODEs and our further work proved that. However, as discussed, the parameter D is restricted by other constants in the model and there is no physical interpretation for this case.

Introducing a spatial component to a basic SIR model spread also naturally explains why areas of high population density experience higher infection rates than more rural areas (for related approaches see e.g. [10, 39]. We also generalized the

concept of the reproduction number in this spatially variable setting, by deriving an eigenvalue problem (5.1), whose solution describes overall decay or spread of the disease. Importantly, the relevant eigenvalue problem near the maximum of the susceptible population can be approximated by a quantum harmonic oscillator which allows an approximate analytical expression for the critical clearance rate that would avoid the spreading of infection. We have tested the relevant predictions numerically, finding very good agreement with our theoretical results, where appropriate.

Aside from spatially-dependent infection rates, our model demonstrates the difficulty of suppressing the outbreaks. As illustrated in Figure 6.2, the disease can "tunnel" between "islands" of positive growth separated by areas of negative growth (i.e., decay) of the epidemic. A better understanding and more systematic quantification of such phenomena is planned for future work.

There are also numerous additional dimensions in which the present consideration can be extended (both literally and figuratively). Indeed, here we restricted considerations to one-dimensional settings, i.e., "geographic corridors". In line with other works such as [9, 27][15, 24], it is naturally more relevant to explore two-dimensional domains. Another assumption was that individuals could only travel to adjacent points, which restricts the value of parameter D. The idea can be generalized if we assume that individuals can travel to all points, and depending on how we will define the travel pattern of individuals, different models can be obtained. For example, a reasonable assumption is that the ratio of population in the destination or the distance between destination and original point determines the rate of travel. We expect that these kind of models enable us to study the situation when diffusion rate D is very large. The goal of travels can be sorted in more generalized model. Although the assumption of returning individuals to their main point seems to be reasonable within appropriate time scale, it can not reflect all daily lives activities. Considering mobility reports of people during Covid-19 pandemic (like reports announced by Google [1]), there are multiple types of travels, and in order to match the theory with reality, different scenarios are needed to be discussed, and considering a scenario that people will not return to their origin seems to be essential. Defining the constants of the equations (e.g. β, γ) as a function of time can be helpful to study

[1] https://www.google.com/covid19/mobility/

the model in smaller time scale. In addition, it is of substantial interest to consider infections across different age groups. Our considerations herein have assumed that the infectiousness and especially recovery properties of the entire population are the same, however it is well-understood that COVID-19 has a far more severe impact on more senior individuals with weakened immune system; indeed, this has been the basis for designing relevant non-pharmaceutical intervention strategies [40]. It is then of interest to introduce kernels of interaction across a "synthetic dimension" representing age (in addition to spatial dimensions). There, interactions are predominant along the "diagonal" i.e., for people of the same age group, but there are nontrivial interactions between age groups at some "distance" between them (e.g., parents/grand-parents and children/grand-children); see, e.g., [41]. There, a more complicated non-monotonic kernel of interaction across ages may be relevant to include. As discussed we started with the basic compartments or SIR model. Adding more compartments which takes the incubation period of the disease, asymptomatically infected individuals, deaths due to the disease separately, vaccinated population and etc, into consideration would help us to develop more reliable model that reflects the reality. This model will lead us to adopt effective policies during the outbreak to save more lives while minimize the effects of restrictions on daily lives. We expect that our results and understanding of infectious disease and epidemiology, can be extended to other applications of compartmental models. For example cancer epidemiology [42], and many other applications that similar models can be applied.

These are all interesting possibilities, currently under consideration for future work and will be reported accordingly in future publications.

Bibliography

[1] Nan Zhang, Pengcheng Zhao, and Yuguo Li. Increased infection severity in downstream cities in infectious disease transmission and tourists surveillance analysis. *Journal of Theoretical Biology*, 470:20–29, 2019.

[2] Oro-Maxillofacial Health and The arctic university of Norway Epidemiology research group. Oro-maxillofacial health and epidemiology.

[3] Nicholas C. Grassly Christophe Fraser. Mathematical models of infectious disease transmission. *Nature Reviews Microbiology*, 6:804–817, 2008.

[4] Norman TJ Bailey et al. *The mathematical theory of infectious diseases and its applications*. Charles Griffin & Company Ltd 5a Crendon Street, High Wycombe, Bucks HP13 6LE., 2nd edition, 1975.

[5] R. Anderson R. May. *Infectious diseases of humans: dynamics and control*. Oxford University Press, Oxford, 1991.

[6] Carlos Castillo-Chavez Fred Brauer. *Mathematical Models in Population Biology and Epidemiology*. Springer, New York, NY, 2001.

[7] Inger Fabris-Rotelli Raeesa Manjoo-Docrat Jennifer Holloway Charl Janse van Rensburg Pravesh Debba Nontembeko Dudeni-Tlhone Zaid Kimmie Alize le Roux Renate Thiede, Nada Abdelatif. Spatial variation in the basic reproduction number of covid-19: A systematic review. *arxiv*, 2020.

[8] Wen TH. Ng, TC. Spatially adjusted time-varying reproductive numbers: Understanding the geographical expansion of urban dengue outbreaks. *Sci Rep 9*, 2019.

[9] P. G. Kevrekidis, J. Cuevas-Maraver, Y. Drossinos, Z. Rapti, and G. A. Kevrekidis. Reaction-diffusion spatial modeling of covid-19: Greece and andalusia as case examples. *Phys. Rev. E*, 104:024412, Aug 2021.

[10] Hao Hu, Karima Nigmatulina, and Philip Eckhoff. The scaling of contact rates with population density for the infectious disease models. *Mathematical Biosciences*, 244(2):125–134, 2013.

[11] Andrea L. Bertozzi, Elisa Franco, George Mohler, Martin B. Short, and Daniel Sledge. The challenges of modeling and forecasting the spread of covid-19. *arXiv*, 2020.

[12] Stephen M. Kissler, Christine Tedijanto, Edward Goldstein, Yonatan H. Grad, and Marc Lipsitch. Projecting the transmission dynamics of sars-cov-2 through the postpandemic period. *Science*, 368(6493):860–868, 2020.

[13] Lia Humphrey, Edward W. Thommes, Roie Fields, Laurent Coudeville, Naseem Hakim, Ayman Chit, and Monica G. Cojocaru. Testing, tracing and social distancing: assessing options for the control of $COVID_19$. *medRxiv*, 2020.

[14] Yingcun Xia, Ottar N. Bjørnstad, and Bryan T. Grenfell. Measles metapopulation dynamics: A gravity model for epidemiological coupling and dynamics. *The American Naturalist*, 164(2):267–281, 2004. PMID: 15278849.

[15] Davide Faranda and Tommaso Alberti. Modeling the second wave of covid-19 infections in france and italy via a stochastic seir model. *Chaos: An Interdisciplinary Journal of Nonlinear Science*, 30(11):111101, 2020.

[16] Hamish McCallum, Nigel Barlow, and Jim Hone. How should pathogen transmission be modelled? *Trends in Ecology Evolution*, 16(6):295–300, 2001.

[17] Gemma Nedjati-Gilani Natsuko Imai Kylie Ainslie Marc Baguelin Sangeeta Bhatia Adhiratha Boonyasiri Zulma Cucunubá-Gina Cuomo-Dannenburg Amy Dighe Ilaria Dorigatti Han Fu Katy Gaythorpe Will Green Arran Hamlet Wes Hinsley Lucy C Okell Sabine van Elsland Hayley Thompson Robert Verity Erik Volz Haowei Wang Yuanrong Wang Patrick GT Walker Caroline Walters Peter Winskill Charles Whittaker Christl A Donnelly Steven Riley Azra C Ghani Neil M Ferguson, Daniel Laydon. Report 9: Impact of non-pharmaceutical interventions (npis) to reduce covid19 mortality and healthcare demand, 2020.

[18] José J Ramasco-Pablo Jensen Vittoria Colizza Andrea Apolloni, Chiara Poletto. The scaling of contact rates with population density for the infectious disease models. *Theoretical Biology and Medical Modelling*, 11(3), 2014.

[19] David Iron Theodore Kolokolnikov Chunyi Gai. Localized outbreaks in an s-i-r model with diffusion. *Journal of Mathematical Biology*, 80:1389–1411, 2020.

[20] Dongmei Chen. *Modeling the Spread of Infectious Diseases: A Review*, chapter 2, pages 19–42. John Wiley Sons, Ltd, 2014.

[21] Vittoria Colizza and Alessandro Vespignani. Epidemic modeling in metapopulation systems with heterogeneous coupling pattern: Theory and simulations. *Journal of Theoretical Biology*, 251(3):450–467, 2008.

[22] Daniela Calvetti, Alexander P. Hoover, Johnie Rose, and Erkki Somersalo. Metapopulation network models for understanding, predicting, and managing the coronavirus disease covid-19. *Frontiers in Physics*, 8:261, 2020.

[23] Yanbo Zhang Xinyue Chen Guiqing Yao Zhangang Han Jiang Zhang, Lei Dong. Investigating time, strength, and duration of measures in controlling the spread of covid-19 using a networked meta-population model. *Nonlinear Dynamics*, 101(3):1789–1800, 2020.

[24] Bin Chen Yimeng Song Tao Zhang Wan Yang Jeffrey Shaman Ruiyun Li, Sen Pei. Substantial undocumented infection facilitates the rapid dissemination of novel coronavirus (sars-cov-2). *Science*, 368(6490):489–493, 2020.

[25] Francesc Aràndiga, Antonio Baeza, Isabel Cordero-Carrión, Rosa Donat, M. Carmen Martí, Pep Mulet, and Dionisio F. Yáñez. A spatial-temporal model for the evolution of the covid-19 pandemic in spain including mobility. *Mathematics*, 8(10), 2020.

[26] Alex Arenas, Wesley Cota, Jesús Gómez-Gardeñes, Sergio Gómez, Clara Granell, Joan T. Matamalas, David Soriano-Paños, and Benjamin Steinegger. Modeling the spatiotemporal epidemic spreading of covid-19 and the impact of mobility and social distancing interventions. *Phys. Rev. X*, 10:041055, Dec 2020.

[27] Ferdinando Auricchio Davide Baroli Thomas J R Hughes Alessia Patton Alessandro Reali Thomas E Yankeelov Alessandro Veneziani Alex Viguerie, Guillermo Lorenzo. Simulating the spread of covid-19 via a spatially-resolved susceptible-exposed-infected-recovered-deceased (seird) model with heterogeneous diffusion. *Appl Math Lett.*, 111, Jan 2021.

[28] Youcef Mammeri. A reaction-diffusion system to better comprehend the unlockdown: Application of seir-type model with diffusion to the spatial spread of covid-19 in france. *Computational and Mathematical Biophysics*, 8(1):102–113, 2020.

[29] Van Kinh Nguyen, Frank Klawonn, Rafael Mikolajczyk, and Esteban A. Hernandez-Vargas. Analysis of practical identifiability of a viral infection model. *PLOS ONE*, 11(12):1–16, 12 2016.

[30] J. Cuevas-Maraver, P.G. Kevrekidis, Q.Y. Chen, G.A. Kevrekidis, Víctor Villalobos-Daniel, Z. Rapti, and Y. Drossinos. Lockdown measures and their impact on single- and two-age-structured epidemic model for the covid-19 outbreak in mexico. *Mathematical Biosciences*, 336:108590, 2021.

[31] Theodore Kolokolnikov Arvin Vaziry and Panayotis G. Kevrekidis. Modelling of spatial infection spread through heterogeneous population: from lattice to pde models. *arxiv*, 2021.

[32] Muhammad Abdullahi Yau. *Analysis of spatial dynamics and time delays in epidemic models*. PhD thesis, University of Sussex, August 2014.

[33] M. B. Short, M. R. D'Orsogna, V. B. Pasour, G. E. Tita, P. J. Brantigham, A. L. Bertozzi, and L. B. Chayes. A statistical model of criminal behavior. *Mathematical Models and Methods in Applied Sciences*, 18(supp01):1249–1267, 2008.

[34] E. E. Holmes, M. A. Lewis, J. E. Banks, and R. R. Veit. Partial differential equations in ecology: Spatial interactions and population dynamics. *Ecology*, 75(1):17–29.

[35] Y. Drossinos Z. Rapti G.A. Kevrekidis P.G. Kevrekidis, J. Cuevas-Maraver. Reaction-diffusion spatial modeling of covid-19: Greece and andalusia as case examples. *arxiv*, 2020.

[36] Analysis of the fisher-kpp equation with a time-dependent allee effect. *IOP SciNotes*, 1(2), 2020.

[37] Jack Xin. Front propagation in heterogeneous media. *SIAM Review*, 42(2):161–230, 2000.

[38] James D. Murray. *Mathematical Biology*. Springer, New York, NY, 3rd edition, 2002.

[39] Theodore Kolokolnikov and David Iron. Law of mass action and saturation in sir model with application to coronavirus modelling. *Infectious Disease Modelling*, 6:91–97, 2021.

[40] P.G. Kevrekidis A. S. Fokas, J. Cuevas-Maraver. Easing covid-19 lockdown measures while protecting the older restricts the deaths to the level of the full lockdown. *Scientific Reports*, 11(5839), 2021.

[41] Laura P. Schaposnik Vishaal Ram. A modified age-structured sir model for covid-19 type viruses. *Scientific Reports*, 11(15194), 2021.

[42] S Franceschi M Plummer I Baussano. Infection transmission and chronic disease models in the study of infection-associated cancers. *British Journal of Cancer*, 110:7–11, 2014.